Dynamical diffraction of guided electromagnetic waves by two-dimensional periodic dielectric gratings

O. Francescangeli and S. Melone

Dipartimento di Scienze dei Materiali e della Terra, Università di Ancona, via Brecce Bianche, I-60131 Ancona, Italy

R. De Leo

Dipartimento di Elettronica e Automatica, Università di Ancona, via Brecce Bianche, I-60131 Ancona, Italy

The properties connected to the propagation of electromagnetic waves in rectangular waveguides loaded by periodic dielectric gratings have been treated by extending the theory of dynamical scattering by perfect atomic crystals. The theoretical formulation has been developed for the TE_{10} excitation of the periodic load, but it remains valid in the same form when a TE_{n0} ($n > 1$) excitation takes place. The analysis was first developed for two-dimensional periodicities, and later the results were applied to one-dimensional periodicities without modifications to the formalism. The generalization of Bragg's law to guided propagation has been obtained, and the conditions and limits of applicability of the theory have been discussed. It has been shown that, when a small permittivity contrast between supporting and loaded material is present, the electromagnetic field can be approximated by either one or two waves only. The expressions of the electromagnetic field supported by the periodic medium and the dispersion relation have been obtained. The diffraction pattern, the deviation from the generalized Bragg law, the width of the total reflection range, and the extinction length have been evaluated for a regular array of cylindrical holes on a polyethylene support. We have reported the results of an experiment carried out to verify the accuracy of the theory. The comparison between theoretical and experimental results has shown excellent agreement.

I. INTRODUCTION

The theory of dynamical scattering (DST) has been extensively used to describe a variety of effects connected to the diffraction of x-rays, neutrons, and electrons by crystals.[1-22] The properties connected to light diffraction by cholesteric liquid crystals were explained by means of the DST (Refs. 23–25) and an application to light diffraction by colloidal crystals was suggested.[26] Recently an extension of the theory has been proposed by the present authors for the diffraction of electromagnetic waves by periodic dielectric media, in a general form valid for a wide frequency range, but with a particular interest in the field of microwaves and millimeter waves.[27] By considering the periodic structure as a macroscopic crystal lattice, the theory makes possible a meaningful physical interpretation of the propagation in terms of incident and diffracted waves. The work of Ref. 27 defines conditions and limits of the applicability of the theory in the form developed, and points out some interesting effects connected with the coupling between incident and diffracted waves. The theoretical forecasts have been successfully verified by means of an experiment involving the propagation of microwaves in a two-dimensional periodic medium inside a parallel-plate waveguide under cutoff, so as to simulate the propagation of plane waves in an unbounded media.

The aim of the present paper is to show that the DST can be successfully extended to the propagation of guided electromagnetic waves in closed structures loaded at periodic intervals with identical dielectric obstacles. The propagation of electromagnetic radiation in guiding periodic structures (waveguides and transmission lines periodically loaded) is a subject of interest due to some interesting and potentially useful properties both in the microwave field[28-30] and, more recently, in the optical field.[31] These include, in particular, the passband-stopband characteristics and the ability to support waves with phase velocities much less than the velocity of light. The passband-stopband characteristics are connected with the existence of frequency bands throughout which the wave propagates without attenuation along the structure, separated by frequency bands throughout which the wave is cut off and does not propagate, a property of interest for its frequency filtering aspects.

The rectangular waveguide is the most commonly used in microwave circuits and our analysis will be limited to it. Nevertheless, the essential properties of hollow cylindrical waveguides are the same, so that an understanding of the diffraction process in rectangular guides may provide suggestions for a more general extension of the dynamical approach to different closed waveguides. The theoretical formulation is developed for the case where the periodic structure is fed by the fundamental mode TE_{10} of the rectangular waveguide. This is the case of interest in most applications since waveguides are typically employed in single-mode propagation regime.

In contrast to the free space and the open waveguides, the hollow closed waveguides do not support the propagation of TEM waves. Their normal modes consist of the TE and TM confined modes with wave vectors belonging

to a discrete set of values. This fact gives the guided propagation a peculiar character, which makes the extension of the DST an original and interesting problem. It will be shown that it is still possible to discuss the coupling of the modes in terms of incident and diffracted waves following the basic lines of the theory developed for the propagation of electromagnetic radiation in unbounded periodic media.[27] This fact confirms once more the power of the dynamical approach in the description of the phenomena connected to the diffraction of waves (matter and electromagnetic waves) by periodic structures. On the other hand, it offers a simple and physically meaningful instrument to study the guided propagation in periodically perturbed media in rectangular waveguides.

Concerning the propagation in unbounded periodic media, exact solutions, in some cases, are available. This is the case, for instance, of the periodic layered media discussed in Refs. 32 and 33. Rigorous theories based on the differential equation approach have also been developed for the diffraction of electromagnetic waves from gratings with one,[34,36] two,[37] and three periodic grating vectors,[38−40] but their application in the general case is rather complex and requires efficient computer numerical calculations. On the other hand, no general theory providing exact solutions is available in the literature for the propagation of electromagnetic radiation in periodically loaded closed waveguides. The approach commonly used makes use of a circuit model involving the construction of an equivalent network for a single basic section (or unit cell) of the structure, followed by an analysis to determine the voltage and current waves that may propagate along the transmission line obtained by the cascade connection of an infinite number of the basic networks.[29] It is also possible to consider a wave-analysis approach,[29] in terms of the forward- and backward-propagating waves existing in each unit cell, which makes use of the wave-amplitude transmission matrix and Floquet's theorem. In both cases, a complete characterization of the periodic load of the unit cell in terms of a shunt susceptance is required, which is a matter of some complexity in the general case and is often possible only in particular cases and/or in approximate forms.

When the periodic load is realized by means of dielectric obstacles, which is the case of interest, approximate solutions of the propagation equation can also be obtained by the coupled-mode theory.[31] That is a general approach where the periodic variation of the dielectric constant is viewed as a perturbation that couples the unperturbed normal modes of the structure. The electric-field vector of the electromagnetic wave is expressed by means of a superimposition of the normal modes of the unperturbed dielectric structure, with unknown amplitude coefficients satisfying a set of coupled linear differential equations. The solution is possible only in an approximate form, when a limited number of modes are strongly coupled ("resonant coupling"). However, the application of the theory requires the perturbed part of the dielectric constant to possess only one-dimensional periodicity, along the axis of the waveguide.

The theory proposed in this paper, on the contrary, is valid for the more general case of two-dimensional periodicities of the dielectric constant. The possibility of a two-dimensional periodicity is important as it offers one more degree of freedom in the design of periodically loaded guiding systems. Differently from the coupled-mode theory, the present approach leads to a set of algebraic linear equations for the amplitudes of the modes coupled by the periodic perturbation. Furthermore, it provides a clear physical insight to the mode coupling and to the condition of weak perturbation, which defines the limits of applicability of the approximations involved. It shows the existence of interesting effects, such as the total reflection, the deviation from the Bragg law, the so-called "pendulum solution."[8] Finally, it allows for the introduction of a characteristic length of the periodic structure (the extinction length), which gives a measure of the length necessary for a strong coupling between incident and diffracted wave to take place.

II. THEORETICAL APPROACH

A. Preliminary considerations

The theory is at first developed for the case of two-dimensional periodicities. At the tend of Sec. II E the results obtained in the following will be applied to one-dimensional periodical structures without any modification of the formalism.

Consider a rectangular waveguide, with cross-section dimensions a and b $(a > b)$, completely filled with a periodic medium consisting of a dielectric substratum, with dielectric constant ϵ_1, which supports a two-dimensional regular array of dielectric cylindrical rods, with dielectric constant ϵ_2. For the magnetic permeability it is assumed that $\mu_1 \simeq \mu_2 \simeq \mu_0$ and both dielectrics are supposed to be without losses. Because of the different dielectric constants with respect to the dielectric matrix, the rods act as scattering elements. A cross section of the waveguide is schematically shown in Fig. 1(a), and Fig. 1(b) shows a top view of the structure. The propagation of the electromagnetic field in a periodic medium is governed by the following differential equation for the displacement vector $\mathbf{D}$:[27]

$$\nabla^2 \mathbf{D} + \nabla \times \nabla \times (\Psi \mathbf{D}) = \epsilon_1 \mu_0 \frac{\partial^2 \mathbf{D}}{\partial t^2}, \qquad (2.1)$$

where

$$\Psi(\mathbf{r}) = 1 - \frac{\epsilon_1}{\epsilon(\mathbf{r})} \qquad (2.2)$$

and the dielectric constant $\epsilon(\mathbf{r})$ has the same periodicity of the lattice.

The problem of the propagation in guiding structures is to find a solution to Eq. (2.1) which satisfies the boundary conditions imposed by the presence of the metallic walls. A significant simplification in the electromagnetic analysis results when we consider the periodic structure fed by the fundamental mode TE_{10} of the unperturbed rectangular waveguide. The electromagnetic problem considered consists in the incidence of a TE_{10} mode (com-
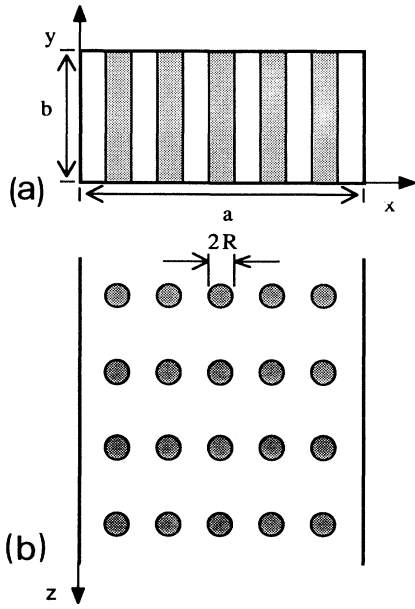
FIG. 1. Schematic picture of the structure investigated. The rectangular waveguide is filled with a two-dimensional periodic dielectric medium consisting of a grating of dielectric cylindrical rods supported by a different dielectric substratum: (a) cross section, (b) top view.

ing from $z = -\infty$) upon the periodic load extending in the region $z > 0$. This approach does not lead to the general solution of the problem, i.e., the general expression of the electromagnetic field supported by the periodic medium, but gives the solution for a particular condition of excitation. This is, in turn, the condition of greatest interest for practical purposes where typically single-mode propagation takes place.

The electromagnetic field in the periodic structure can be expressed in terms of a superposition of normal modes of the unperturbed waveguide. So, in the general case, all TE and TM modes should be considered. However, when a TE_{10} excitation takes place, the y uniformity of both the exciting field and the periodic load makes it impossible for the excitation of modes with field components that are nonuniform in the y direction. Hence all TM and TE_{0m} modes cannot be excited and it is possible to neglect them in the theoretical formulation. On the contrary, all TE_{n0} modes, which possess a y-uniform field distribution, can be excited in the general case (in particular, if the periodic load is symmetric with respect to $x = a/2$, only TE_{n0} modes with n odd are excited). Their only nonzero component of the electric field is parallel to the y axis.

According to the above considerations, in the presence of a TE_{10} excitation, we expect a general solution of Eq. (2.1) for the displacement vector $\mathbf{D}$ of the form

$$\mathbf{D} = \sum_{n=1}^{\infty} \sin(n\pi x/a) D_n(z) \exp[2\pi i(ft - K_n' z)]\mathbf{u}_y \ , \quad (2.3)$$

where f is the frequency of the electromagnetic field, $K_n' = [\epsilon_1 \mu_0 f^2 - (n/2a)^2]^{1/2}$ is the guide wave vector of the

TE_{n0} mode of the unperturbed waveguide, and, due to the periodic nature of the load, $D_n(z)$ is a one-dimensional periodic function

$$D_n(z + ha_1) = D_n(z) \ , \quad h = 0, \pm 1, \pm 2, \ldots \ . \quad (2.4)$$

By expanding $D_n(z)$ in Fourier series, Eq. (2.3) becomes

$$\mathbf{D} = \sum_{n=1}^{\infty} \sum_{h=-\infty}^{\infty} \sin(n\pi x/a) D_{nh} \exp[2\pi i(ft - K_{nh}' z)]\mathbf{u}_y$$

$$(2.5)$$

with

$$K_{nh}' = K_n' + h/a_1 \ , \quad (2.6)$$

which expresses the field in terms of only TE_{n0} modes, with wave vectors related by Eq. (2.6) and coefficients D_{nh} to be determined so as to satisfy Eq. (2.1). Once Eq. (2.1) for the displacement vector $\mathbf{D}$ is solved, the associated magnetic field is obtained from Maxwell's equations.

In the present paper we prefer to follow an alternative way of solving the electromagnetic problem, by introducing an "equivalent" open waveguide (i.e., parallel-plate waveguide), defined in Sec. II B, and first studying the propagation through it. That allows us to introduce some simplifications in the theoretical treatment. As shown in Sec. II D, the solution of the closed waveguide problem can be easily derived from the solution of the two-dimensional open equivalent problem. The propagation in the open structure, in turn, can be studied in the framework of the theory developed by the authors in Ref. 27. This approach also points out that the nature of the mode coupling for the TE_{n0} modes in the periodically loaded rectangular waveguide is just the same as the one which takes place between the plane waves propagating in unbounded periodic media.

B. Solution for the open equivalent structure

Consider a parallel-plate waveguide, infinitely wide in the x direction, with a separation of the conducting plates b, completely filled with the same periodic medium filling the rectangular waveguide. The structure is referred to as an equivalent open waveguide, the sense of the equivalence being clarified in Sec. II D. The unit cell of the rectangular grating is shown in Fig. 2 and is defined by the vectors $\mathbf{a}_1, \mathbf{a}_2$ in real space. The radius of the circular cross section of the cylindrical rods is denoted by R and the origin of the reference system is chosen at a corner of the unit cell.

In the unit cell $\epsilon(\mathbf{r})$ takes the following values:

$$\epsilon(\mathbf{r}) = \begin{cases} \epsilon_1 \ , & |\mathbf{r}| > R \\ \epsilon_2 \ , & |\mathbf{r}| < R \ . \end{cases} \quad (2.7)$$

For this waveguide we consider the electromagnetic problem analogous (or "equivalent") to the one discussed in Sec. II A for the rectangular waveguide. It consists in the determination of the electromagnetic field which rises in the medium when it is excited by the fundamental mode, i.e., the TEM mode for the parallel-plate waveguide. The propagation of a TEM wave through a
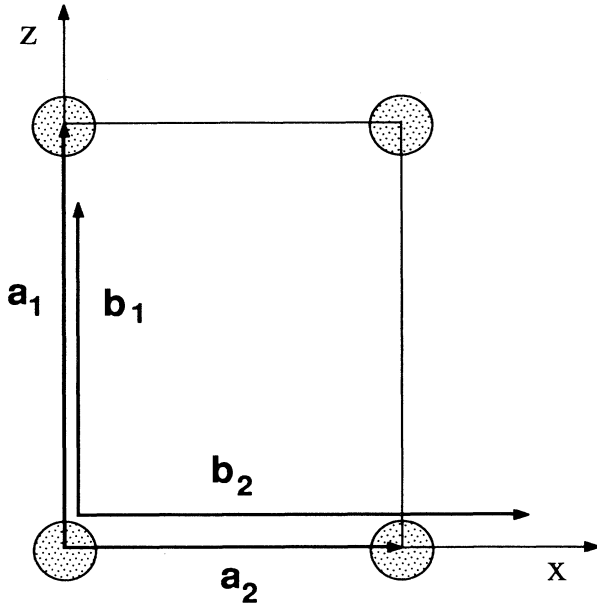
FIG. 2. Unit cell of the periodic grating. a_1 and a_2 define the unit cell in the real space; b_1 and b_2 are the unit vectors of the reciprocal lattice.

y-uniform parallel-plate waveguide is a typical two-dimensional problem. The wave vectors of incident and diffracted waves lie along the x-z plane and all the physical parameters involved are y independent. In fact, the uniformity with y both of the excitation and the periodic load does not allow the propagation of modes with y-dependent field components. No TE and TM mode is then excited by the incident field, but only other TEM waves which can propagate in different directions parallel to the conducting planes. The excited fields have no component of the electric field parallel to the plates of the waveguide, so that the presence of the conducting plates limiting the region of space interested in the propagation is of no relevance in the theoretical treatment. The situation is then equivalent to the propagation of a uniform plane wave (with the electric field along the y axis) through a two-dimensional periodic unbounded medium uniformly extending to infinity in the y direction.

Equation (2.1) still describes the propagation in the two-dimensional media, where r indicates now the position vector in the x-z plane. Because of the periodic nature of the medium, and taking into account the above considerations, the general solution of Eq. (2.1) can be expressed as a linear combination of Bloch waves:[6]

$$D(r) = \sum_H D_H \exp[2\pi i (ft - K_H \cdot r)] , \qquad (2.8)$$

where

$$K_H = K_0 + B_H . \qquad (2.9)$$

K_0 is the wave vector of the internal incident wave. K_0 and K_H lie in the plane xz parallel to the conducting plates and each $D_H = D_H u_y$ is directed along the y axis.

$\Psi(r)$ is a doubly periodic function of r and it can be ex-

panded in the Fourier series:

$$\Psi(r) = \sum_H \Psi_H \exp(-2\pi i B_H \cdot r) \qquad (2.10)$$

with

$$\Psi_H = \frac{1}{S} \int_S \Psi(r) \exp(2\pi i B_H \cdot r) dS , \qquad (2.11)$$

where S is the surface of the unit cell, $B_H = h b_1 + k b_2$ is the two-dimensional reciprocal lattice vector associated with the h, k Miller indices, and b_1 and b_2 are the unit vectors of the reciprocal lattice, defined by the relation $a_i \cdot b_j = \delta_{ij}$ ($i, j = 1, 2$). The vectors b_1 and b_2 are also shown in Fig. 2. The sum over H means all possible values of h, k. Taking into account Eqs. (2.2) and (2.7), the Fourier coefficients (2.11) take the form

$$\Psi_H = \frac{1}{S}(1 - \epsilon_1/\epsilon_2) f_H \qquad (2.12)$$

with

$$f_H = \int_{S_0} \exp(2\pi i B_H \cdot r) dS , \qquad (2.13)$$

where the integration surface S_0 is the circular cross section of the cylindrical rod, corresponding to $|r| \leq R$. Equation (2.13) defines the form factor of the scattering element. The calculation of the integral in Eq. (2.13), by expanding the exponential term in the Taylor series, gives the expression of the form factor f_H in the form of a rapidly convergent series[27]

$$f_H = \sum_{n=0}^{\infty} (-1)^n \frac{(2\pi B_H)^{2n}}{(2n)!} \frac{R^{(2n+2)}}{2n+2} I_{2n} , \qquad (2.14)$$

where

$$I_{2n} = \frac{2n-1}{2n} I_{2n-2} , \quad I_0 = 2\pi . \qquad (2.15)$$

For the more general structure with N scattering elements in the unit cell, centered in r_n ($n = 1, 2, \ldots, N$) and with cross section surface S_n (not necessarily circular), Eq. (2.12) modifies to the form

$$\Psi_H = \frac{1}{S}(1 - \epsilon_1/\epsilon_2) F_H \qquad (2.16)$$

with

$$F_H = \sum_{n=1}^{N} f_{Hn} \exp(2\pi i B_H \cdot r_n) \qquad (2.17)$$

with f_{Hn} the structure factor of the nth scattering element. Equation (2.17) defines the structure factor of the unit cell. The form factor depends only on the geometry of the scatterers, while the structure factor is a function only of their distribution inside the unit cell.

Using Eqs. (2.8) and (2.10) the product ΨD can be written in the form of series

$$\Psi D = \sum_H (\Psi D)_H \exp[2\pi i (ft - K_H \cdot r)] , \qquad (2.18)$$

where the Hth Fourier coefficient is a sum over all the reciprocal lattice points

$$(\Psi \mathbf{D})_H = \sum_L \Psi_{H-L} \mathbf{D}_L \ . \tag{2.19}$$

The insertion of expansions (2.8) and (2.18) into Eq. (2.1), after equating the corresponding Fourier coefficients of the two sides, gives the following infinite set of linear differential equations:

$$(K_H^2 - \epsilon_1 \mu_0 f^2) \mathbf{D}_H = K_H^2 \sum_L \Psi_{H-L} \mathbf{D}_L \ , \tag{2.20}$$

where $f(\epsilon_1 \mu_0)^{1/2} = K$ is the wave vector of a plane wave with frequency f in a homogeneous medium of dielectric constant ϵ_1. A solution of Eqs. (2.20) gives the unknown amplitudes D_H and the related wave vectors K_H.

In analogy with Ref. 9 we define the "resonance error" δ_H by the equation

$$K_H = K(1 + \delta_H) \ . \tag{2.21}$$

When the speed of one or more of the plane waves of expansion (2.8) approaches the speed of the light in the homogeneous medium of dielectric constant ϵ_1, $v = (\epsilon_1 \mu_0)^{-1/2}$, the corresponding resonance errors become small in comparison with unity, and Eq. (2.20) reduces to a close approximation:

$$\mathbf{D}_H = \frac{1}{2\delta_H} \sum_L \Psi_{H-L} \mathbf{D}_L \ . \tag{2.22}$$

The presence of the terms δ_H in the denominator causes a resonance effect which makes the amplitudes of the corresponding waves dominant over all the others. These waves can be taken as an approximation of the total field. In these conditions $|K_H| \simeq K$ and the normal modes of the periodically perturbed structure are close to normal modes of the unperturbed structure. So, as a first approximation, the periodic variation of the dielectric constant can be considered as a perturbation that couples the unperturbed normal modes of the structure, in accordance with the coupled-mode-theory approach. The modal coupling condition is expressed by Eq. (2.9). The situation described occurs when the presence of the periodic grating can be considered as a small perturbation of the homogeneous supporting medium, i.e., when at least one of the two following conditions: $\epsilon_1 \simeq \epsilon_2$ or $\sum_n S_n \ll S$ (with the sum extended to a unit cell), is verified. When this is so, the function $|\Psi(\mathbf{r})|$ is small in comparison with unity "nearly" everywhere inside the unit cell.

The degree of approximation involved in the analysis is related to the values of the resonance errors. The smaller the resonance errors, the more accurate the approximations introduced. In x-ray and neutron diffraction the resonance errors are of the order of 10^{-4}–10^{-5} and sometimes even less. This is a consequence of the smallness of the function $\Psi(\mathbf{r})$, being typically $|\Psi(\mathbf{r})| \simeq 10^{-4}$–$10^{-6}$. In Ref. 27 it has been shown that the two-wave approximation still gives reliable results and with good accuracy when the term $|\Psi_H|$, associated with the Hth reflection, is of the order of 10^{-2}. This is the case of interest in the microwave frequency range[27] and corresponds to resonance errors between 10^{-1} and 10^{-3}. In the millimeter-wavelength range it is possible to obtain values one order of magnitude smaller while still lower values are achieved in the optical frequency range. From this point of view, the condition of small perturbation is equivalent to the presence of coefficients $|\Psi_H|$ equal to or smaller than $\sim 10^{-2}$ or, equivalently, resonance errors lower than 10^{-1}. The directions of the waves of appreciable intensity can be found by using the construction involving the Ewald sphere drawn in the reciprocal space.[9,12,27]

Equation (2.8) gives the general solution to the propagation problem for a parallel-plate waveguide excited by a TEM wave propagating in an arbitrary direction $\mathbf{K}_0$ parallel to the conducting planes. It expresses the fields as a sum of normal modes of the open two-dimensional structure consisting of uniform plane waves with wave vectors in the xz plane and related by Eq. (2.9). To complete the analogy with the rectangular waveguide problem we have to consider the incident TEM mode to propagate along z. Moreover, when the periodic structure is limited to the region $z > 0$, the boundary conditions over the limiting surface $z = 0$ require $\mathbf{D}_H = 0$ for all waves with wave vectors not parallel to the z axis. Equation (2.8) then reduces to

$$\mathbf{D}(z) = \sum_{h=-\infty}^{\infty} \mathbf{D}_h \exp[2\pi i (ft - K_h z)] \tag{2.23}$$

with

$$K_h = K_0 + h b_1 \ , \quad h = 0, \pm 1, \pm 2, \ldots , \tag{2.24}$$

where $\mathbf{K}_0 = K_0 \mathbf{u}_z$ and the vector $\mathbf{B}_H = h \mathbf{b}_1 = \mathbf{B}_h$ ($h = 0, \pm 1, \pm 2, \ldots$) now moves along the direction $\mathbf{b}_1$ of the reciprocal lattice. So, in order to find the solution for the closed structure, it is not necessary in the following to consider the general solution of the parallel-plate waveguide, but it is sufficient to limit the field expansion to the plane-wave terms (2.23) propagating along z and to study the mode-coupling in this direction. On the other hand, according to the equivalence stated in the Sec. II D, expansion (2.23) really gives rise, for the rectangular waveguide, to the general solution of the form expected (2.5). In other terms, the normal modes of the closed periodic structure investigated derive from the plane-wave terms of Eq. (2.8) describing propagation along the waveguide axis z.

Accordingly, we limit our analysis to the one-dimensional solution (2.23) of the propagation equation (2.1). Equations (2.8)–(2.22) are still valid in the same form with $H = (h,k)$ replaced by the index h. In particular, the system (2.22) for the field amplitudes reduces to

$$D_h = \frac{1}{2\delta_h} \sum_{l=-\infty}^{\infty} \Psi_{h-l} D_l \ . \tag{2.25}$$

The mode-coupling can still be described by using the Ewald sphere in the reciprocal lattice, as shown in Fig. 3. The unidirectional character of the propagation involved in the present analysis [Eq. (2.23)] results in the localization of the center of the sphere over axis $\mathbf{b}_1$ of the reciprocal lattice, which is parallel to the direction of propagation z. If $\mathbf{K}_0 = K_0 \mathbf{u}_z$ is the wave vector of the incident wave and $H = (h,0)$ any reciprocal-lattice point on axis
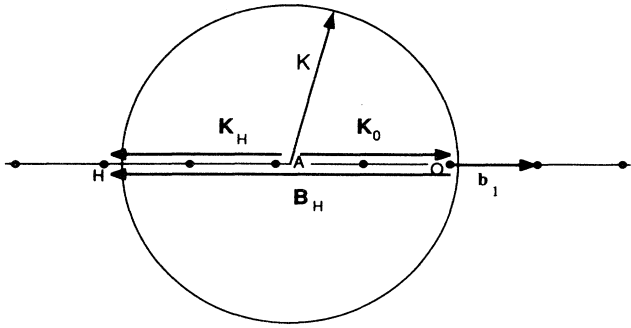
FIG. 3. Ewald sphere in the reciprocal space. O and H are, respectively, the origin and a point of the reciprocal lattice, and A is the center of the sphere. $\mathbf{K}_0$ is the wave vector of the incident wave and $\mathbf{K}_H = \mathbf{K}_0 + \mathbf{B}_H$ the wave vector of the diffracted wave.

$\mathbf{b}_1$ other than 0, then, according to Eqs. (2.23) and (2.24), $\mathbf{K}_H = \mathbf{K}_h = \mathbf{K}_0 + \mathbf{B}_H = (K_0 + hb_1)\mathbf{u}_z$ is the wave vector of a possible constituent wave of the total field. Still, the wave will have appreciable amplitude only if H lies very close to the sphere, thus resulting in a small resonance error. In such a case we speak of "resonant coupling" between the corresponding waves, and the resonance error can be considered as a measure of the degree of wave coupling. The geometrical construction shows that no more than two waves can be resonantly coupled and the coupling, when present, can only be contradirectional, i.e., the incident and the coupled diffracted wave propagate along opposite directions. In this case $|K_h| \simeq |\mathbf{K}_0| \simeq K = 1/\lambda$ and Eq. (2.24) becomes $B_h \sim 2K$, which is very nearly equal to the Bragg diffraction law with grazing angle $\theta = \pi/2$:

$$h\lambda = 2a_1 . \tag{2.26}$$

When no reciprocal-lattice point other than the origin lies near the Ewald sphere, the incident wave will produce diffracted (reflected) waves of negligibly small amplitude and the total field can be approximated by one wave. We can set $D_h = 0$ for $h \neq 0$, and the system (2.25) reduces to the equation

$$\delta_0 = \frac{\Psi_0}{2} = \frac{\sum_n S_n}{2S}(1 - \epsilon_1/\epsilon_2) , \tag{2.27}$$

where the last equality makes use of Eqs. (2.16) and (2.17). The quantity $(1 + \delta_0) = n$ defines the refraction index n of the periodic medium relative to that of the supporting medium.

When another reciprocal-lattice point h, other than the origin, lies near the Ewald sphere, the field is essentially made up of two dominant wave fields. By setting $D_1 = 0$ for $l \neq 0, h$, Eq. (2.25) reduces to the linear homogeneous system

$$(\Psi_0 - 2\delta_0)D_0 + \Psi_{\bar{h}}D_h = 0 ,$$

$$\Psi_h D_0 + (\Psi_0 - 2\delta_h)D_h = 0 , \tag{2.28}$$

where $\bar{h} = -h$. Equations (2.28) have a nontrivial solution only if the determinant vanishes

$$(\Psi_0 - 2\delta_0)(\Psi_0 - 2\delta_h) = |\Psi_h|^2 , \tag{2.29}$$

where we have set $\Psi_{\bar{h}} = (\Psi_h)^*$ as it results from relations (2.16), (2.17), and (2.13). Equation (2.29) is the dispersion equation.

The resonance error δ_h is a function of δ_0, as shown also by the geometrical construction in Fig. 3. Combining Eqs. (2.21) and (2.24) and neglecting the terms δ_l^2 $(l = 0, h)$ with respect to $2\delta_l$, the following linear relation between δ_h and δ_0 can be found:

$$\delta_h = \frac{1}{b}\delta_0 + \frac{\alpha}{2} , \tag{2.30}$$

where

$$\alpha = (B_h^2 - 2KB_h)/K^2 , \tag{2.31}$$

$$1/b = 1 - B_h/K , \tag{2.32}$$

and $B_h = hb_1$. The parameter α is a function of the wavelength deviation from the value λ_B corresponding to the Bragg law.

In particular, for wavelength λ close to λ_B, which is the case of interest, Eq. (2.30) can be written to a close approximation:[6]

$$\alpha = 4(\lambda - \lambda_B)/\lambda_B . \tag{2.33}$$

With the same order of approximation the quantity b reduces to

$$b = -1 . \tag{2.34}$$

It is useful to express the solution of Eq. (2.29) in terms of the dimensionless quantity Y defined by

$$Y = \frac{\Psi_0 - \alpha/2}{|\Psi_h|} = \frac{\Psi_0 - 2(\lambda - \lambda_B)/\lambda_B}{|\Psi_h|} . \tag{2.35}$$

By inserting Eq. (2.30) into Eq. (2.29), one obtains an equation in δ_0, the solution of which can be written

$$\left.\begin{array}{c}\delta_0' \\ \delta_0''\end{array}\right\} = \tfrac{1}{2}\{\Psi_0 + |\Psi_h|[-Y \pm (Y^2 - 1)^{1/2}]\} . \tag{2.36}$$

By introducing the variable $X = D_h/D_0$ and solving the dispersion equation in X, two solutions X_1 and X_2 are obtained:

$$\left.\begin{array}{c}X_1 \\ X_2\end{array}\right\} = \frac{|\Psi_h|[-Y \pm (Y^2 - 1)^{1/2}]}{\Psi_{\bar{h}}} . \tag{2.37}$$

Since there are two possible values for δ_0 and for the amplitude ratio X, there are two internal incident waves and two internal diffracted waves. The general form on the incident wave field inside the medium is thus

$$e^{-2\pi iKz}(D_0'e^{-i\phi_1 z} + D_0''e^{-i\phi_2 z}) \tag{2.38}$$

and for the diffracted wave field

$$e^{2\pi i(B_h - k)z}(X_1 D_0' e^{-i\phi_1 z} + X_2 D_0'' e^{-i\phi_2 z}) , \qquad (2.39)$$

where $\phi_1 = 2\pi K \delta_0'$, $\phi_2 = 2\pi K \delta_0''$. The terms in parentheses in Eqs. (2.38) and (2.39) result in a modulation of the field amplitude along the propagation direction z, which will be discussed in more detail in Sec. II E.

C. Geometrical interpretation

It is possible to give a useful geometrical interpretation of the results obtained in Sec. II B that allows a graphical solution of the dispersion equation. We introduce two variables ζ_0 and ζ_h:

$$\zeta_0 = \delta_0 - \Psi_0/2 , \qquad (2.40)$$

$$\zeta_h = \delta_h - \Psi_0/2 , \qquad (2.41)$$

In terms of these, Eqs. (2.29) and (2.30), respectively, take the forms

$$\zeta_0 \zeta_h = |\Psi_h|^2/4 , \qquad (2.42)$$

$$\zeta_0 + \zeta_h = -y|\Psi_h| . \qquad (2.43)$$

In the plane $\zeta_0 \zeta_h$, Eq. (2.42) defines an equilateral hyperbola with diameter $D_1 D_2 = 2^{1/2}|\Psi_h|$ (the dispersion curve), while Eq. (2.43) represents a straight line with slope -1 and a known term depending on the wavelength λ, as shown in Fig. 4. A given value of λ fixes the intercept of the straight line with axis of the variable Y [defined by Eq. (2.35)] and hence its position in the plane according to the geometrical construction of the figure. The intersections between the hyperbola and the straight
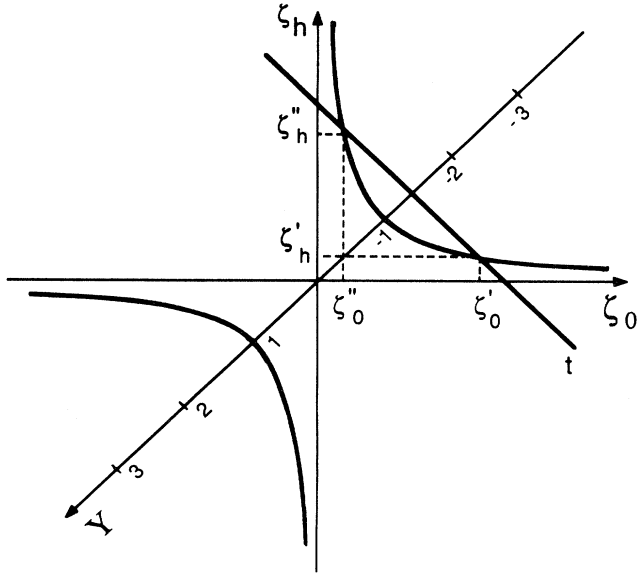
FIG. 4. Geometrical description of the dispersion equation in the plane ζ_0, ζ_h. The equilateral hyperbola is the dispersion curve. The intersections between the curve and the straight line t give the solutions to the dispersion equation. Y is the dimensionless parameter defined by Eq. (2.35) and its axis lies on the bisector line of the first and third quadrants.

line give, according to Eqs. (2.40) and (2.41), the solution δ_0, δ_h to the dispersion equation. It is also possible to obtain a geometrical solution for the amplitude ratio X in terms of ζ_0, ζ_h by observing that, according to Eqs. (2.28),

$$X = D_h/D_0 = 2\zeta_0/\Psi_{\bar{h}} = \Psi_h/2\zeta_h .$$

The picture clearly shows the existence of a wavelength range, corresponding to the interval $|Y| < 1$, where no intersection takes place and consequently no real solution for δ_0 is obtained. This situation corresponds to the excitation of evanescent waves, with consequent total reflection of the incident radiation. The total reflection range coincides with the forbidden band of the classical electromagnetic theory of periodic media. In the range $|Y| > 1$ two distinct solutions are obtained and the geometrical construction shows that it is always $\delta_0' = \delta_h''$ and $\delta_0'' = \delta_h'$. Furthermore, it shows that the difference $(\zeta_0' - \zeta_0'') = (\zeta_h'' - \zeta_h')$ in the values of the two solutions increases with $|Y|$ and this is relevant in connection with the period of the above-mentioned spatial modulation of the field amplitude, which is related to such difference.

D. Equivalence between the parallel plate and rectangular waveguide

In Sec. II B we discussed the solutions to the propagation problem for the parallel-plate waveguide. We found that the field expressed by Eq. (2.23), with coefficients D_h satisfying Eq. (2.25), is a solution for the propagation along the z direction. When resonant coupling takes place, a limited number of waves, with wave vectors $|K_h| \sim K$, are considered and D becomes an explicit function of K. The field $\mathbf{D} = D(z, \mathbf{K})\mathbf{u}_y$ satisfies the propagation equation (2.1), which, by expanding the term $\nabla \times \nabla \times (\Psi \mathbf{D}) = -\nabla^2(\Psi \mathbf{D}) + \nabla \nabla \cdot (\Psi \mathbf{D})$ and considering that $\nabla \cdot (\Psi \mathbf{D}) = 0$, can be written in the equivalent form

$$[(1 - \Psi)\nabla^2 + 4\pi^2 K^2 - \nabla^2 \Psi]\mathbf{D} = 0 . \qquad (2.44)$$

Referring to the reference system of Fig. 1, we consider now the derived field

$$\mathbf{D}' = \sin(n\pi x/a)D(z, K')\mathbf{u}_y . \qquad (2.45)$$

By definition the term $D(z, K')\mathbf{u}_y$ satisfies Eq. (2.44) with K' instead of K. On using this result and neglecting $\Psi(\mathbf{r})$ with respect to unity, according to the considerations in Sec. II B concerning the smallness of the function $|\Psi(\mathbf{r})|$, the propagation Eq. (2.44) for $\mathbf{D}'$ reduces to

$$[K^2 - K'^2 - (n/2a)^2]\mathbf{D}' = 0 . \qquad (2.46)$$

Hence, to satisfy Eq. (2.46), we require that

$$K' = [K^2 - (n/2a)^2]^{1/2} . \qquad (2.47)$$

Provided that K' has this value, Eq. (2.45) describes a field that is a solution of the propagation equation and satisfies the boundary conditions at $x = 0, a$. It is therefore appropriate to represent the field in a waveguide with parameter a fed by a mode of the form $\sin(n\pi x/a)$. This result indicates that if an appropriate solution of the electric field is found for a periodically loaded parallel-plate region, the corresponding waveguide solution is found by replacing K by K' everywhere, and multiplying

the electric field by $\sin(n\pi x/a)$. The associated magnetic field is then found from Maxwell's equations. By summing the terms (2.45) over all integers n ($n = 1,2,\ldots$), it is easily seen that the general solution has the form expressed by Eqs. (2.5) and (2.6), as anticipated in Sec. II B.

If the waveguide is fed by the fundamental TE_{10} mode and single-mode propagation takes place, which is the case of interest, then $n = 1$ and $K' = [K^2 - (1/2a)^2]^{1/2}$. The introduction of K' instead of K is equivalent to substituting the free-space wavelength $\lambda = 1/K$ by the corresponding TE_{10} mode guide wavelength $\lambda' = 1/K'$, related to λ by the relation

$$\lambda' = \lambda/[1 - (\lambda/2a)^2]^{1/2} . \tag{2.48}$$

Accordingly, the whole formulation of the theory and all the considerations of the preceding sections concerning the wave coupling, the geometrical constructions involving the Ewald sphere and the dispersion curve remain valid in the same form provided λ is replaced by λ'. In particular, the resonant coupling condition, i.e., Bragg's law, is now expressed in terms of the guide wavelength λ' in the form

$$2d = n\lambda' , \quad n = 1,2,3,\ldots \tag{2.49}$$

where $d = 1/|B_h|$ is the interplanar distance of the family of planes corresponding to the reflection B_h. Equation (2.49) can be considered the generalization of the Bragg law (in backscattering condition) for the guided propagation, where the free-space wavelength is replaced by the guide wavelength. We will refer to it as the guide Bragg law.

Finally, the parameter Y, on which wave amplitudes and resonance errors depend, is expressed by

$$Y = \frac{\Psi_0 - 2(\lambda' - \lambda'_B)/\lambda'_B}{|\Psi_h|} , \tag{2.50}$$

where λ'_B is the guide wavelength value that satisfies the guide Bragg law.

E. Solution for the rectangular waveguide

When resonant coupling takes place the electric field in the rectangular waveguide fed by the fundamental TE_{10} mode is obtained from Eqs. (2.38) and (2.39) according to the results of Sec. II D. The expressions of the electric field of the incident and reflected waves are, respectively,

$$E^+ = \sin(\pi x/a)e^{-2\pi i K'z}(E'_0 e^{-i\phi_1 z} + E''_0 e^{-i\phi_2 z}) , \tag{2.51}$$

$$E^- = \sin(\pi x/a)e^{2\pi i(2K'_B - K')z}$$
$$\times (X_1 E'_0 e^{-i\phi_1 z} + X_2 E''_0 e^{-i\phi_2 z}) , \tag{2.52}$$

where

$$(2K'_B - K') = 2/\lambda'_B - 1/\lambda' \simeq 1/\lambda' = K', \quad \phi_1 = 2\pi K'\delta'_0 ,$$

$$\phi_2 = 2\pi K'\delta''_0, \quad E'_0 = D'_0/\epsilon_1, \quad E''_0 = D''_0/\epsilon_1 .$$

The last two equalities follow from the consideration that, in the presence of a small perturbation, the relation

$D = \epsilon_1 E$ is valid "nearly everywhere" inside the unit cell, as discussed in Sec. II B. The magnetic field is then obtained from Maxwell's equations

$$H_x^\pm = (-i/\omega\mu_0)\frac{\partial E^\pm}{\partial z} , \tag{2.53}$$

$$H_z^\pm = (i\pi/\omega\mu_0 a)\cotan(\pi x/a)E^\pm , \tag{2.54}$$

where $\omega = 2\pi f$ and E^+ and E^- are, respectively, given by Eqs. (2.51) and (2.52). After introducing Eq. (2.51) into Eq. (2.53) we obtain

$$H_x^+ = -\frac{2\pi K'}{\omega\mu}\frac{(1+\delta'_0)E'_0 e^{-i\phi_1 z} + (1+\delta''_0)E''_0 e^{-i\phi_2 z}}{E'_0 e^{-i\phi_1 z} + E''_0 e^{-i\phi_2 z}}E^+ . \tag{2.55}$$

Equation (2.55) can be simplified by noting that the resonance errors are small with respect to unity, thus resulting in a close approximation

$$H_x^\pm = \pm(-2\pi K'/\omega\mu)E^\pm , \tag{2.56}$$

where the result of the analogous calculation for H_x^- is also reported. Each of the two waves, incident and diffracted, coupled by the periodic perturbation consists in the superimposition of two TE_{10} modes with wave vectors close to K' (the wave vector of the fundamental mode in the unperturbed waveguide), but slightly different from each other. The associated spatial beat results in a modulation of the amplitude of the resulting wave along the direction of propagation, as shown clearly in the following.

The approximation leading to Eq. (2.56) is equivalent to neglecting the slow spatial variation of the electric-field amplitude $A(z)$ associated with the spatial beat, that is $|dA(z)/dz| \ll |2\pi K' A(z)|$. It is possible to show that, for small resonance errors, $|d^2 A(z)/dz^2| \ll |2\pi K' dA(z)/dz|$, also results which is known as parabolic approximation and is used to characterize "weak perturbations" in the framework of the coupled-mode theory.[31] The electromagnetic field expressed by Eqs. (2.51)–(2.54) gives the general solution to the propagation problem when the periodic medium is unlimited in both directions $\pm z$, so that no boundary condition need be assumed. If we consider a portion, limited by two parallel-plane surfaces in $z = 0,L$ and a feeding TE_{10} mode incident in $z = 0$, by imposing the boundary conditions over the limiting surfaces, it is possible to determine the amplitudes of the excited fields and the diffraction pattern, i.e., the ratio between the diffracted and the incident power. If we suppose the waveguide filled with supporting medium in the region $z < 0$ and $z > L$, the boundary conditions for the electric field in $z = 0$ and L become, respectively,

$$E'_0 + E''_0 = E_0 , \tag{2.57}$$

$$c_1 x_1 E'_0 + c_2 x_2 E''_0 = 0 , \tag{2.58}$$

where $c_1 = \exp(-i\phi_1 L)$, $c_2 = \exp(-i\phi_2 L)$, and E_0 is the electric-field amplitude of the incident TE_{10} mode. In Eq.

(2.57) the reflection at interface $z = 0$ has been neglected since the refraction index of the periodic medium is very close to that of the supporting medium. Equation (2.58) follows the consideration that the diffracted wave emerges through the boundary $z = 0$ while it must vanish at the boundary $z = L$.[6] After solving Eqs. (2.57) and (2.58) the electric fields of the incident and diffracted waves take the forms

$$E^+ = E_0 \sin(\pi x/a) e^{-i2\pi K_B' z} \frac{Y \sinh[A(1-Y^2)^{1/2}(L-z)/L] - i(1-Y^2)^{1/2}\cosh[A(1-Y^2)^{1/2}(L-z)/L]}{Y\sinh[A(1-Y^2)^{1/2}] - i(1-Y^2)^{1/2}\cosh[A(1-Y^2)^{1/2}]} , \quad (2.59)$$

$$E^- = E_0 \sin(\pi x/a) e^{i2\pi K_B' z} \frac{-\sinh[A(1-Y^2)^{1/2}(L-z)/L]}{Y\sinh[A(1-Y^2)^{1/2}] - i(1-Y^2)^{1/2}\cosh[A(1-Y^2)^{1/2}]} \frac{|\Psi_h|}{\Psi_{\bar{h}}} \quad (2.60)$$

for $|Y| \leq 1$, and

$$E^+ = E_0 \sin(\pi x/a) e^{-i2\pi K_B' z} \frac{(Y^2-1)^{1/2}\cos[A(Y^2-1)^{1/2}(L-z)/L] + iY\sin[A(Y^2-1)^{1/2}(L-z)/L]}{(Y^2-1)^{1/2}\cos[A(Y^2-1)^{1/2}] + iY\sin[A(Y^2-1)^{1/2}]} , \quad (2.61)$$

$$E^- = E_0 \sin(\pi x/a) e^{i2\pi K_B' z} \frac{-i\sin[A(Y^2-1)^{1/2}(L-z)/L]}{(Y^2-1)^{1/2}\cos[A(Y^2-1)^{1/2}] + iY\sin[A(Y^2-1)^{1/2}]} \frac{|\Psi_h|}{\Psi_{\bar{h}}} \quad (2.62)$$

for $|Y| \geq 1$, where $K_B' = 1/\lambda_B'$ and $A = \pi K'L|\Psi_h|$ is a dimensionless parameter depending on the structure factor and on the overall length L of the periodic medium.

From Eq. (2.56) it follows that the Poynting vector is proportional to the square of the electric field. If we suppose the external incident TE_{10} mode normalized to a power flow of 1 W in the z direction, then the power flow of the incident and diffracted (reflected) waves is given, respectively, by $P_i(z) = |A_i(z)|^2$ and $P_r(z) = |A_r(z)|^2$, where $A_i(z)$ are $A_r(z)$ are the z-dependent terms of the relative amplitudes. In the wavelength range corresponding to $|Y| \leq 1$ we obtain

$$P_i(z) = \frac{\cosh^2[A(1-Y^2)^{1/2}(L-z)/L] - Y^2}{\cosh^2[A(1-Y^2)^{1/2}] - Y^2} , \quad (2.63)$$

$$P_r(z) = \frac{\sinh^2[A(1-Y^2)^{1/2}(L-z)/L]}{\cosh^2[A(1-Y^2)^{1/2}] - Y^2} . \quad (2.64)$$

For sufficiently large arguments of the hyperbolic-cosine and hyperbolic-sine functions, the incident mode power drops off exponentially in the perturbation region. This behavior is due not to absorption, but to the reflection of power into the backward-traveling mode, and corresponds to the excitation of evanescent waves. Equations (2.63) and (2.64) satisfy the relation $P_i(L) + P_r(0) = 1$ and the net power flow in the z direction $[P_i(z) - P_r(z)]$ is constant with z. Both the conditions are consistent with the conservation of energy. A plot of the mode powers $P_i(z)$, and $P_r(z)$ as a function of z for this case is shown in Fig. 5. The dashed line (the two curves for P_i and P_r are superimposed) is plotted for $Y = 0.5$ and for a value $A = 9.83$, corresponding to the experimental situation described in Sec. III. In this case the length of the periodic medium is $L = 181.2$ cm and corresponds to a ratio $L/L_{ex} = 5.33$, L_{ex} being the "extinction length" discussed in more detail in the following. The solid lines in the same figure are relative to the values $Y = 0.5$ and $A = 1.84$, corresponding to a value L equal to one extinction length. An inspection of expressions (2.63) and (2.64) or, equivalently, Fig. 5 shows an important feature connected with the total reflection regime. At a given frequency in the total reflection range ($|Y| < 1$), the penetration depth of the fields inside the periodic medium tends to a limit value with increasing L, which depends on the frequency and on the structure factor. Once we define the penetration η depth as the value of z corresponding to an attenuation of the electromagnetic field of a factor $1/e$ with respect to the value at the input surface, we find

$$\eta = \frac{\lambda'}{\pi|\Psi_h|(1-Y^2)^{1/2}} . \quad (2.65)$$

The power exchange between the two coupled modes in the region between $z = 0$ and L is given by $P_r(0) = |A_r(0)|^2$, as it can be seen in Fig. 5, where the
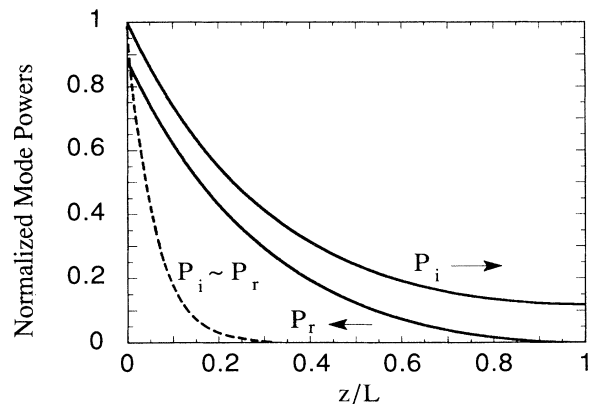
FIG. 5. Mode powers of the incident and reflected modes in the periodic dielectric medium as a function of the depth z for a frequency in the total reflection range. The solid lines refer to $Y = 0.5$ and $A = 1.84$. The dashed line is relative to $Y = 0.5$ and $A = 9.83$, where the two curves for the incident and reflected powers are superimposed. The arrows indicate the direction of propagation along the z axis.

mode power exchange as a function of z is well evident. We note that the fractional power exchange decreases as Y increases and a complete exchange only occurs when $Y = 0$, a condition close to but not exactly equal to the guide Bragg diffraction law, as shown in more detail in the following. Out of this condition, a complete exchange is possible only for large values of L (see the dashed line).

In the range corresponding to $|Y| \geq 1$ we have

$$P_i(z) = \frac{Y^2 - \cos^2[A(Y^2-1)^{1/2}(L-z)/L]}{Y^2 - \cos^2[A(Y^2-1)^{1/2}]} \; , \qquad (2.66)$$

$$P_r(z) = \frac{\sin^2[A(Y^2-1)^{1/2}(L-z)/L]}{Y^2 - \cos^2[A(Y^2-1)^{1/2}]} \; . \qquad (2.67)$$

Again, $P_i(L) + P_r(0) = 1$, results and the net power flow in the z direction is independent of z. The behavior of the mode powers as a function of z, for this case, is shown in Fig. 6. The figure refers to the experimental situation of Sec. III, with $Y = 2$. The solution expressed by Eqs. (2.66) and (2.67) involves sinusoidal oscillations and is referred to as "pendulum solution" in the theory of x-ray diffraction by crystals. It is a consequence of the spatial beat between the two modes which make up the field, both the incident and reflected ones. The period Λ of the spatial beat depends, in particular, on the frequency of the electromagnetic radiation and is given by

$$\Lambda = \frac{\lambda'}{|\Psi_h|(Y^2-1)^{1/2}} \; . \qquad (2.68)$$

The reflectivity R is defined as the ratio of the reflected to the incident power $P_r(0)/P_i(0) = |A_r(0)/A_i(0)|^2$ and according to Eqs. (2.63), (2.64), (2.66), and (2.67) is given by

$$R = \frac{\sinh^2[A(1-Y^2)^{1/2}]}{\cosh^2[A(1-Y^2)^{1/2}] - Y^2} \; , \qquad |Y| \leq 1 \qquad (2.69)$$
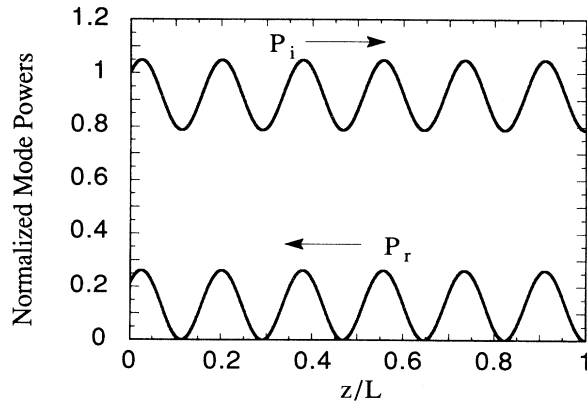
FIG. 6. Mode powers of the incident and reflected modes in the periodic dielectric medium as a function of the depth z for a frequency out of the total reflection range ($Y = 2$). The curves are plotted for numerical values corresponding to the experimental situation described in Sec. III. The arrows indicate the direction of propagation along the z axis.

$$R = \frac{\sin^2[A(Y^2-1)^{1/2}]}{Y^2 - \cos^2[A(Y^2-1)^{1/2}]} \; , \qquad |Y| \geq 1 . \qquad (2.70)$$

A typical plot of the calculated reflectivity as a function of Y and for different lengths of the periodic medium is shown in Fig. 2 of Ref. 27. The spectrum consists of a main peak centered in $Y = 0$, with a sharp cutoff (for sufficiently high L) and a series of sidelobes. An effect of total reflection is evident in the range $|Y| \leq 1$ with increasing L (the "Darwin width" in the theory of x-ray diffraction by perfect crystals), as shown clearly also by Eq. (2.69). The guide wavelength range corresponding to total reflection is found by using Eq. (2.50),

$$\Delta\lambda' = \lambda'_B|\Psi_h| \; . \qquad (2.71)$$

The corresponding frequency range can be found by using the relation between λ' and f,

$$\lambda' = \frac{v/f}{[1-(v/2af)^2]^{1/2}} \; , \qquad (2.72)$$

following from Eq. (2.48). The full width at half maximum (FWHM) of the diffraction peak corresponds to the range $|Y| \leq 2/\sqrt{3}$ in the Y domain[6] and, according to Eqs. (2.50) and (2.72), to the frequency range

$$\Delta f = v \left[\left[\frac{1}{\lambda'^2_1} + \frac{1}{4a^2} \right]^{1/2} - \left[\frac{1}{\lambda'^2_2} + \frac{1}{4a^2} \right]^{1/2} \right] \; , \qquad (2.73)$$

where $\lambda'_{2,1} = \lambda'_B(1 + \Psi_0/2 \pm |\Psi_h|/\sqrt{3})$. The peak value of the reflectivity occurs in $Y = 0$ and its position is very close to the center of the pattern. On the wavelength scale its position, according to Eq. (2.50), is given by

$$\lambda'_C = \lambda'_B(1 + \Psi_0/2) \; . \qquad (2.74)$$

This equation shows that the peak of the diffraction pattern does not coincide with the guide wavelength λ'_B corresponding to the guide Bragg law. The deviation from the guide Bragg law $(\lambda'_C - \lambda'_B)$ may be positive or negative depending upon the sign of Ψ_0. This effect is a consequence of the refraction, which causes the guide wavelength in the periodic medium to be slightly different from the guide wavelength in the homogeneous substratum by the relative refraction index factor $n = 1 + \delta_0 = 1 + \Psi_0/2$. Equation (2.74) is a confirmation of this fact and shows that the guide Bragg law is exactly satisfied when the guide wavelength in the periodic medium λ'_C is considered.

From Eq. (2.21) with $H = 0$, which gives the wave vector of the internal incident wave, and Eqs. (2.36) and (2.50), we find the following relation between the propagation constant in the periodic medium K'_p and the frequency f:

$$K'_p = K'(\lambda'/\lambda'_B \pm \{[\lambda'/\lambda'_B - (1 + \Psi_0/2)]^2 - |\Psi_h|^2/4\}^{1/2}) \; , \qquad (2.75)$$

where $K' = 1/\lambda'$ and λ' is related to the frequency according to Eq. (2.72). Figure 7 shows the dispersion relation $\omega(K'_p)$ [obtained from Eqs. (2.72) and (2.75) with $\omega = 2\pi f$] close to the frequency corresponding to the oc-
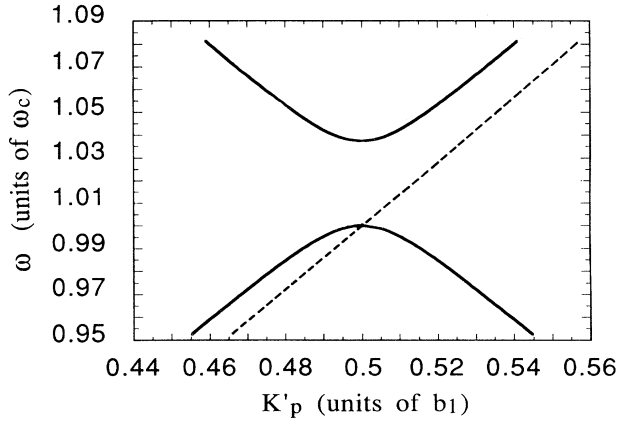
FIG. 7. Dispersion relation $\omega(K_p')$ near a forbidden band (solid line). The dispersion relation is plotted for the periodic structure of the experiment described in Sec. III. The angular frequency ω is normalized to the value ω_c, corresponding to the center of the total reflection range. The dashed line represents the wave vector of the fundamental mode in the unperturbed waveguide.

currence of diffraction. The curve is plotted for particular numerical values of the constants Ψ_0 and $|\Psi_h|$, corresponding to the experimental condition described in Sec. III, but its behavior is quite general. Two values of the wave vector correspond to each frequency out of the stopband range, one of which is close to the K', the wave vector of the unperturbed waveguide (shown in Fig. 7 by the dashed line).

Figure 7 shows that the group velocity $v_g = d\omega/dK_p'$ progressively reduces to zero as the edges of the passband are approached. We note that for a range of frequencies such that $|\lambda'/\lambda_B' - (1+\Psi_0/2)| < |\Psi_h|/2$, K_p' has an imaginary part. This is the "forbidden" region, in which the evanescent behavior shown in Fig. 5 occurs and which is formally analogous to the energy gap in semiconductors when the periodic crystal potentials causes the electron propagation constant to become complex.

Finally, we introduce the extinction length defined as the length of the periodic structure above which the integrated intensity $\int R(Y)dY$ differs from its asymptotic value π (for L tending to infinite) in a quantity less than 5%,[6]

$$L_{ex} = \frac{\lambda_B'}{\sqrt{\pi}|\Psi_h|} \; . \tag{2.76}$$

It is a measure of the length necessary for a strong-coupling interaction between incident and diffracted wave to set up. For a thickness L of the periodic layer smaller than L_{ex}, a "kinetic" approach that neglects the extinction of the primary wave and the multiple-scattering effects is possible and sufficiently accurate.[6] With increasing L, the coupling between incident and diffracted wave becomes more and more important and the dynamical approach is necessary to describe the experimental evidences.

The extinction length and the penetration depth are related quantities. In particular, at the peak of the forbid-

den band ($Y = 0$) the simple relation holds

$$L_{ex} = \sqrt{\pi\eta} \; . \tag{2.77}$$

The peculiar effects expected by the DST can be considered to take place when the thickness L is a few extinction lengths.

In microwave frequency range and with coefficients $|\Psi_h|$ of the order of 10^{-2}, values of a few tens of centimeters are obtained for the extinction length. In a millimeter-wave frequency range, values smaller than one order of magnitude can be obtained with the same resonance errors, while in the optical field values of a few tens of micrometers can be achieved, which makes the application in this field particularly attractive.

In conclusion, a brief discussion of one-dimensional periodicities is reported, in connection with the important role played by the periodic layered media in integrated optics. The simplest periodic layered medium consists of two different materials with a dielectric constant profile given by

$$\epsilon(\mathbf{r}) = \begin{cases} \epsilon_2 \; , & |z| < d/2 \\ \epsilon_1 \; , & d/2 < |z| < a_1/2 \end{cases} \tag{2.78}$$

with

$$\epsilon(z) = \epsilon(z + a_1) \; , \tag{2.79}$$

where the z axis is normal to the layer interfaces and a_1 is the period. The treatment of this simple case shows how to apply the previous results to one-dimensional periodicities. An extension to more complex geometries is then immediate.

The unit cell in the real space is defined by the vector $\mathbf{a}_1 = a_1 \mathbf{u}_z$, while $\mathbf{b}_1 = (1/a_1)\mathbf{u}_z$ defines the unit cell in the one-dimensional reciprocal lattice. A vector $\mathbf{B}_h$ of the reciprocal lattice is expressed by $\mathbf{B}_h = (h/a_1)\mathbf{u}_z$ ($h = 0, \pm 1, \pm 2, \dots$).

$\Psi(\mathbf{r})$ is now a periodic function of the only variable z and the following expression of the coefficient Ψ_h is obtained:

$$\Psi_h = \frac{d}{a_1}(1 - \epsilon_1/\epsilon_2)\frac{\sin(h\pi d/a_1)}{(h\pi d/a_1)} \; . \tag{2.80}$$

Once the expressions of the coefficients Ψ_h are determined, the rest of the analysis developed in the preceding sections remains unchanged in the form. It can be shown that the results obtained with this approach for the expressions of the electromagnetic fields, the diffraction pattern, and the width of the forbidden band are in very good agreement with the results that can be obtained by the application of the coupled-mode theory.

III. EXPERIMENTAL SETUP

We carried out an experiment in order to verify the theoretical predictions and to evaluate the accuracy of the DST in the form proposed. In particular, the aim of the experiment was to measure the diffraction pattern around a diffraction peak, to show the presence of the total reflection effect, to measure the width of the total

reflection range, and to verify the deviation from the guide Bragg law.

The experiment was realized with a standard X-band rectangular waveguide ($a = 2.286$ cm, $b = 1.016$ cm). The measurements were performed in the microwave frequency range 7.4–8.6 GHz with a step of 3 MHz, which is the maximum frequency resolution allowed by the analyzer in the range of the measurement. The lower value of the range was chosen so as to work sufficiently above the cutoff frequency of the fundamental TE_{10} mode $f_{10} = 6.557$ GHz. In the frequency range of the measurement single-mode propagation takes place. In fact, the symmetry of the TE_{10} excitation field and of the periodic load makes impossible the excitation of the first higher-order mode TE_{20}, whose cutoff frequency in the dielectric matrix ($f_{20} = 8.564$ GHz) is slightly lower than the upper limit of the measurement range. Moreover, all the other higher-order modes have cutoff frequencies greater than 8.6 GHz.

The rectangular waveguide, of overall length 230 cm, was realized in aluminum 11S, which allowed good mechanical processing, and the dielectric supporting medium was in polyethylene. The measured relative dielectric constant of the polyethylene was found to be flat over a wide range of frequency. For the real part we measured $\epsilon_1' = 2.345$ and for the dissipation factor ϵ_1''/ϵ_1' we obtained a value lower than 10^{-3}. Due to the small value of the dissipation factor the dielectric losses can be neglected.

The periodic structure consists of a two-dimensional grating of cylindrical holes with circular cross section, made on the dielectric support. The lattice spacings are $a_1 = 15.1$ mm, $a_2 = 3.1$ mm, and the radius of the circular hole is $R = 0.75$ mm. The unit cell contains only one cylindrical hole centered at the origin and according to Eq. (2.12), the coefficients Ψ_0 and Ψ_h, respectively, take the form

$$\Psi_0 = \frac{\pi R^2}{a_1 a_2} \left[1 - \frac{\epsilon_1}{\epsilon_2} \right] , \qquad (3.1)$$

$$\Psi_h = \frac{1}{a_1 a_2} \left[1 - \frac{\epsilon_1}{\epsilon_2} \right] f_h , \qquad (3.2)$$

with f_h calculated according to Eq. (2.14). By inserting the numerical values of the quantities we obtain $\Psi_0 = -5.0776 \times 10^{-2}$ and $\Psi_h = -5.0160 \times 10^{-2}$.

The grating was realized by a computer-aided machine and consists of 120 rows, each of them containing 7 holes, for a total number of 840 scattering elements in an overall length of 181.2 cm. The extinction length calculated according to Eq. (2.76) is found to be $t_{ExB} = 33.97$ cm, so that the length of the periodic structure corresponds to 5.33 extinction lengths.

A schematic picture of the experimental equipment is shown in Fig. 8. The periodically loaded waveguide is fed by the microwave power source through a coaxial cable and a matched standard coaxial-waveguide transition. This is introduced to match the coaxial cable to the empty rectangular waveguide and it allows us to reduce the reflection coefficient of the transition to values lower than -30 dB over the entire frequency range of interest. In the reflection measurement configuration, the 230-cm-long aluminum waveguide containing the dielectric grating is terminated on a standard matched load. It acts as an absorbing termination and avoids the reflection of the transmitted power (the reflection coefficient is lower than -50 dB). In the transmission measurement configuration the output of the aluminum waveguide is connected to the second port of the analyzer through a coaxial cable and a second matched coaxial-waveguide transition identical to the input one.
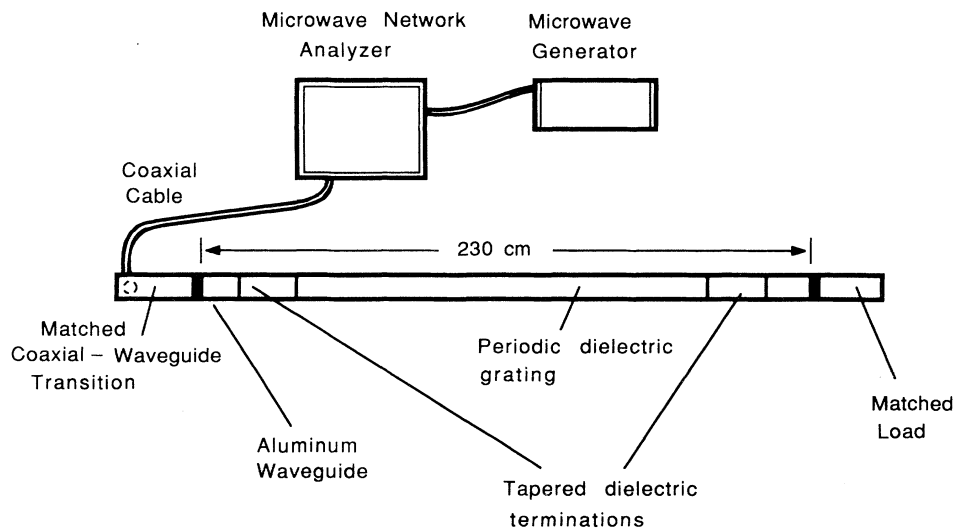
FIG. 8. Schematic picture of the experimental setup in the configuration for the measurement of the reflection coefficient. In the configuration for transmission coefficient measurements, the matched load is replaced by a matched coaxial-waveguide transition connected, through a coaxial cable, to the second port of the analyzer.

The measurements were performed with the microwave network analyzer HP8510 and the calibration of the instrument was carried out at the terminal ports of the aluminum waveguide. The analyzer has two input-output connections which make it possible to measure the reflection coefficient at the two calibration ports and the port-to-port transmission coefficients. To reduce the mismatch associated with the discontinuity of the dielectric constant between the empty space and the dielectric substratum, the dielectric bar was not abruptly truncated at the edges, but it was tapered to a wedge-shaped profile. In this way the reflection at the interface becomes negligible in accordance with the theory developed. The distance between the shaped profile and the periodic load is enough to make all the excited higher-order modes strongly attenuated at the input surface of the periodic medium.

In the configuration for reflection coefficient measurements (Fig. 8) the reflected wave field coming back to the instrument is separated from the incident one by the directional coupler of the analyzer and it is possible to measure the reflection coefficient $\Gamma = [|A_r(0)| / A_i(0)]$, the square of which gives the diffraction pattern $[P_r(0)/P_i(0)]$.

IV. RESULTS AND DISCUSSION

The measured reflection coefficient of the periodic structure as a function of frequency is shown by the heavy solid line in Fig. 9. The thin solid line in the same figure represents the theoretical reflection coefficient calculated by Eqs. (2.59)–(2.62). A high-reflectivity frequency range, corresponding to the total reflection range, is well evident in the experimental pattern, together with the presence of secondary maxima, as expected by the theory.

Excellent agreement can be observed between the two
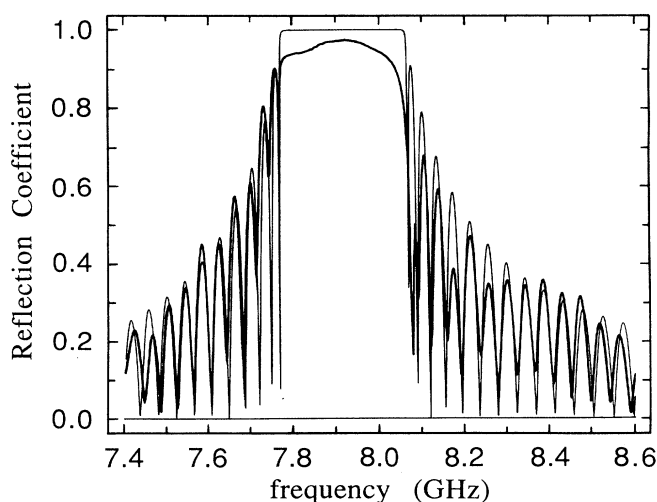
FIG. 9. Reflection coefficient of the periodically loaded rectangular waveguide of Fig. 8 as a function of frequency. The thin solid line represents the theoretical pattern, the heavy solid line shows the experimental result.

patterns. In particular, concerning the positions of the peaks, we note that in the theoretical pattern the main peak is centered at a frequency $f = 7.915$ GHz and in the experimental curve the center, measured as the middle point between the two minima of the peak, corresponds to a frequency $f = 7.913$ GHz with an error of only 0.03%, which is smaller than the experimental resolution. The very good coincidence in the position of the main peak is the direct proof of the effect of deviation from the guide Bragg law. The center of the peak, according to the Bragg law, should occur at $f = 7.769$ GHz, thus resulting in a theoretical deviation of 146 MHz, a value that is in excellent agreement with the value $\Delta f = 144$ MHz, which experimentally measured. A very good result is found also for the positions of the sidelobes. Apart from the first one close to the main peak on the right-hand side of the pattern, which is not clearly resolved, the peaks in the theoretical and experimental patterns are substantially superimposed in the frequency range 7.5–8.5 GHz. Only a small but progressively increasing shift of the positions seems to appear for the farther peaks close to the upper and lower limits of the frequency measurement band. Still the maximum deviation is very small, corresponding to a relative error of about 0.2%. This behavior can be justified by observing that the approximations involved in the theory, in particular, in the derivation of the linear relation between δ_h and δ_0, are accurate in a limited frequency range close to the central peak and their accuracy progressively fails with increasing the frequency deviation (from the central value). The experimental results show that the theory gives very good results in a frequency range of 1 GHz around the central frequency $f = 7.91$ GHz, which corresponds to a relatively high value of the relative deviation $(\Delta f / f)100$ of approximately 13%. Out of this frequency range, a better agreement could, in principle, be obtained by removing, in the theoretical treatment of Sec. II B, the assumption $\delta_h^2 \ll \delta_h$, which progressively begins to fail as the frequency deviation from the central value increases (because of the frequency dependence of the resonance errors). This approach leads to a fourth-order dispersion equation in δ_0,[19] which results in incident and diffracted wave fields made up of four waves. Still, the considerable increase in the analytical treatment and the very good quality of the present results do not justify the introduction of such a refinement, at least for the frequency range investigated.

The main peak in the experimental pattern is close to the theoretical unitary value, but it results a little lower (with a maximum value of 0.97) and it is not perfectly flat in the range corresponding to total reflection. This is a consequence of the conduction losses associated with the finite conductivity of the waveguide walls, which, in contrast to the dielectric losses, are not negligible. We measured the conduction losses for the empty waveguide by the measurement of the transmission coefficient. This was not sufficient, however, to make a correction for the conduction losses of the experimental curve since the current distribution on the waveguide walls is considerable different in the two situations. On the other hand, a theoretical calculation of the losses which takes into ac-
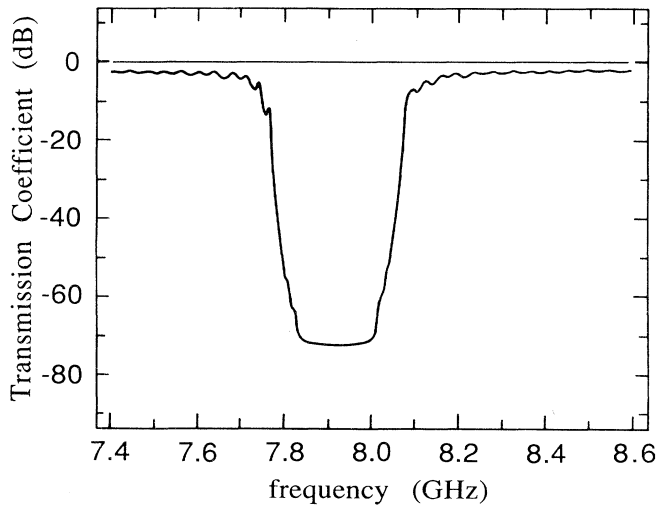
FIG. 10. Transmission coefficient in logarithmic scale (dB) as a function of frequency.

count the actual current distribution appears particularly complicated since the losses are not sufficiently small to justify the classical first-order theoretical approach for the determination of the attenuation constant.[28] Still, if we suppose, as a first approximation, that the losses in the loaded waveguide are not notably different from those of the empty waveguide, we find that the attenuation is enough to account for the lower value of the experimental peak reflectivity.

The theoretical total reflection range (Darwin width), calculated by Eqs. (2.71) and (2.72) or measured from the pattern of Fig. 9, is 288 MHz. The slight smoothing of the central peak in the experimental pattern associated with the losses makes the singling out of the Darwin range and the measurement of its width difficult. On the other hand, we can compare the FWHM of the experimental and theoretical reflection peaks. According to Eq. (2.73) we find a value $\Delta f = 333$ MHz, for the FWHM of the theoretical pattern, which agrees very well with the value $\Delta f = 335$ MHz measured in the experimental pattern. The small residual discrepancy between theoretical and experimental pattern, consisting in the flexible monotone behavior of the sidelobe amplitudes, is mostly due to background associated with the imperfect match of the tapered dielectric terminations.

Finally, Fig. 10 reports the transmission coefficient $[\,|A_i(L)|\,|A_i(0)|\,]$ in logarithmic scale (dB) as a function of the frequency, obtained by measuring the ratio of the transmitted field amplitude to the incident field amplitude with the experimental equipment in the transmission measurement configuration. This figure shows the very good quality of the investigated structure as a stopband filter, due to the sharp cutoff and to the high attenuation level in a wide frequency range (about -70 dB in a range of about 180 MHz).

V. CONCLUSIONS

The proposed theory extends the basic ideas of the DST, developed for free propagation in unbounded periodic media, to the propagation of electromagnetic radiation in closed periodic guiding structures. It provides a simple instrument to approximate the electromagnetic field when the periodic can be considered as a small perturbation. The conditions and the limits of applicability of the theory have been treated and in particular the degree of the modal coupling and the entity of the perturbation have been quantitatively discussed in terms of the resonance error.

The theoretical formulation has been developed for the TE_{10} excitation of the rectangular waveguide, but it is valid also for TE_{n0} excitations. In fact, it is easily seen from the theory of Sec. II B and II D that if a TE_{n0} ($n > 1$) can propagate in the waveguide, the electromagnetic field excited in the periodic medium is readily obtained from Eqs. (2.38) and (2.39) by multiplying the field amplitudes by $\sin(n\pi x/a)$ and replacing K by the guide wave vector of the TE_{n0} mode of the unperturbed waveguide [Eq. (2.47)]. The results of Sec. II E apply, in the same forms, to TE_{n0} modes. A more general formulation of the theory, which gives the general solution for the electromagnetic field supported by the periodic medium including TM and TE_{0m} modes, is another subject of investigation by the present authors.

The theoretical treatment has been developed for two-dimensional periodicities, and afterward the theory has been applied to one-dimensional geometries where a very good agreement with the results of the coupled-mode theory can be found. The generalization of the Bragg law to the guided propagation, as the condition for modal coupling between incident and diffracted waves, has been obtained.

The experimental results show very good agreement with the theory. In connection with the conclusions made in Ref. 27, this fact can be considered as a further confirmation of the validity of the theory in the case when the resonance errors are of the order of 10^{-2}.

The subject of the present paper is of interest both from a general physics and an applied point of view. On the one hand, the proposed extension of the DST shows once more the power of the dynamical approach in the study of the phenomena connected to the diffraction by periodic structures, both in free and guided propagation. This is a meaningful result due to the peculiar character of guided propagation with respect to free propagation. On the other hand, the structures studied are characterized by some properties which make them interesting for applications in the microwave and millimeter-wave field. These are connected, in particular, to the possibility of realizing filtering devices and slow-wave structures.

A further extension of the theory to dielectric waveguides would be of interest in the optical field, where the phenomena connected to the propagation of light in periodic dielectric media are employed in many optical devices such as diffraction gratings, holograms, free-electron lasers, distributed-feedback lasers, distributed-Bragg-reflector lasers, high-reflectance Bragg mirrors,

acousto-optic filters, and so on. Nevertheless, the theory, as an extension of the DST, suggests the possibility that other interesting effects known for x-ray, neutron, and electron diffraction by crystals, such as the Bormann effect, the Pendellösung effect, the Fanckuchen effect, and the angular amplification,[9,11,18] could have applications in these fields. In these directions, further investigations are currently in progress by the present authors.

[1] C. G. Darwin, Philos. Mag. 27, 315 (1914); 27, 675 (1914).

[2] P. P. Ewald, Ann. Phys. (Leipzig) 49, 1 (1916).

[3] P. P. Ewald, Ann. Phys. (Leipzig) 49, 117 (1916).

[4] P. P. Ewald, Ann. Phys. (Leipzig) 54, 519 (1917).

[5] M. Laue, Ergeb. Exakten Naturwiss. 10, 133 (1931).

[6] W. H. Zachariasen, Theory of X-Ray Diffraction in Crystals (Wiley, New York, 1945).

[7] M. von Laue, Materiewellen und Interferenzen (Akademic Verlagsges, Leipzig, 1948).

[8] N. Kato, J. Phys. Soc. Jpn. 7, 397 (1952).

[9] R. W. James, in Solid State Physics, edited by F. H. Seitz and D. E. Turnbull (Academic, New York, 1953), Vol. 15, pp. 53–220.

[10] P. P. Ewald, Acta Crystallogr. 11, 888 (1958).

[11] G. Bormann, in Trends in Atomic Physics, edited by O. R. Frish et al. (Interscience, New York, 1959).

[12] B. W. Battermann and H. Cole, Rev. Mod. Phys. 36, 681 (1964).

[13] P. P. Ewald, Rev. Mod. Phys. 37, 46 (1965).

[14] C. G. Shull, Phys. Rev. Lett. 21, 1585 (1968).

[15] N. Kato, in Introduction to X-Ray Crystallography, edited by L. V. Azaroff (McGraw-Hill, New York, 1974).

[16] R. Colella, Acta Cryst. A 30, 413 (1974).

[17] M. L. Colberger and F. Seitz, Phys. Rev. 71, 294 (1974).

[18] Z. G. Pinsker, Dynamical Scattering of X-Rays in Crystals (Springer-Verlag, Berlin, 1978).

[19] R. W. James, The Optical Principles of the Diffraction of X-Rays, (Ox Bow, Woodbridge, CT, 1982).

[20] P. L. Cowan, Phys. Rev. B 32, 5437 (1985).

[21] S. M. Durbin and T. Gog, Acta Cryst. A 45, 132 (1989).

[22] F. Rieutord, Acta Cryst. A 46, 526 (1989).

[23] S. Chandrasekhar and K. N. Srinivasa Rao, Acta Cryst. A 24, 445 (1968).

[24] S. Mazkedian, S. Melone, and F. Rustichelli, Phys. Rev. A 14, 1190 (1976).

[25] V. A. Belyakov and V. D. Dmitrienko, Fiz. Tverd. Tela (Leningrad) 15, 2724 (1974) [Sov. Phys.—Solid State 15, 1811 (1974)].

[26] S. Melone and F. Rustichelli, Solid State Commun. 55, 97 (1985).

[27] O. Francescangeli, S. Melone, and R. De Leo, Phys. Rev. A 40, 4988 (1989).

[28] R. E. Collin, Field Theory of Guided Waves (McGraw-Hill, New York, 1960).

[29] R. E. Collin, Foundations for Microwave Engineering (McGraw-Hill KogaKusha, Tokyo, 1966).

[30] R. H. Bevensee, Electromagnetic Slow Wave Systems (Wiley, New York, 1964).

[31] A. Yariv and P. Yeh, Optical Waves in Crystals (Wiley-Interscience, New York, 1984), and references quoted therein.

[32] F. Abeles, Ann. Phys. (Paris) 5, 596 (1950); Thin Films 5, 706 (1950).

[33] P. Yeh, A. Yariv and C. -S. Hong, J. Opt. Soc. Am. 67, 423 (1977); A. Yariv and P. Yeh, J. Opt. Soc. Am. 61, 438 (1977).

[34] M. S. Moharam and T. K. Gaylord, J. Opt. Soc. Am. 71, 811 (1981).

[35] Z. Zylberberg and E. Maron, J. Opt. Soc. Am. 73, 392 (1983).

[36] K. Rokushina and J. Yamakita, J. Opt. Soc. Am. 73, 901 (1983).

[37] S. P. Liu, Proc. Natl. Sci. Counc. (Repub. China) A 9, 163 (1985); S. P. Liu and Y. T. Cheng, J. Opt. Eng. (Repub. China) 3, 1 (1986).

[38] S. P. Liu, Proc. Nat. Sci. Counc. (Repub. China) A 10, 26 (1986); 10, 173(E) (1986).

[39] S. P. Liu, Chin. J. Phys. (Taipei) 24, 54 (1986).

[40] S. P. Liu, Phys. Rev. B 39, 10 640 (1989).